Determining Conversion Gain and Read Noise Using a Photon-Counting Histogram Method for Deep Sub-Electron Read Noise Image Sensors

DAKOTA A. STARKEY (Student Member, IEEE), AND ERIC R. FOSSUM (Fellow, IEEE)

Thayer School of Engineering at Dartmouth, Hanover, NH 03755, USA

CORRESPONDING AUTHOR: E. R. FOSSUM (e-mail: eric.r.fossum@dartmouth.edu)

ABSTRACT A new method for characterizing deep sub-electron read noise image sensors is reported. This method, based on the photon-counting histogram, can provide easy, independent and simultaneous measurements of the quanta exposure, conversion gain, and read noise. This new method provides a more accurate measure of conversion gain and read noise over conventional characterization techniques for image sensors with read noise from 0.15–0.40e- rms.

INDEX TERMS CMOS image sensor, photon counting, low read noise, conversion gain, VPR, VPM, PCH, DSERN.

I. INTRODUCTION

Conversion gain and read noise are two important figures of merit for high-sensitivity image sensors, due to their impact on the signal-to-noise ratio. Characterizing these properties involves the use of multiple methodologies such as the photon transfer curve (PTC) [1]–[3] and noise analysis of dark measurements [4]. It is important that these methods be accurate, as error in this calculation will propagate through any other calculations that use these values.

The PTC is typically used to extract the conversion gain of an image sensor by exploiting the nominally linear relationship between photon-shot-noise-induced signal variance and signal mean. It is assumed the signal variance is only due to shot noise, and is equal to the mean of the signal, resulting in a linear region that is limited by the linear full well capacity (FWC) of the pixel. When the PTC is used to extract the conversion gain on a pixel by pixel basis, a large number of frames over a wide range of signal levels are needed, and the best overall linear fit usually ignores any non-linearity in the data. It is worth noting that a linear fit can also be obtained from a log-noise vs. log-mean plot; however, small errors in the slope and intercept can produce large errors in the extracted conversion gain so this technique is not recommended.

Read noise is an inherent property of image sensors and is caused primarily by the thermal and 1/f noise of the readout transistors, making it mostly signal independent. Correlated double sampling (CDS) is often used to suppress the read noise, but some noise always remains. To determine the read noise, many dark frames are taken and the temporal standard deviation of all the frames is calculated. For this method to be accurate, the integration time of the sensor needs to be as short as possible to limit the effect of dark current. By operating at the minimum integration time, the sensor is forced to use artificial timing that may change the read noise of the sensor. Cooling to reduce dark current would also change the intrinsic read noise.

The recent development and emergence of deep-sub-electron-read noise (DSERN) photon-counting quanta image sensors [5], [6], where the read noise is less than 0.5e- rms, suggests a new method of testing called the photon-counting histogram (PCH) [7], [8]. Using this method, conversion gain and read noise of DSERN image sensors can be characterized using a single test. The PCH method relies on the statistical model presented in [9], which is applicable for DSERN devices. DESRN devices have been previously demonstrated using either avalanche gain or multiple readouts at low temperature (e.g., [10] and [11]). While these works discuss using the single-photon resolution of the sensor to
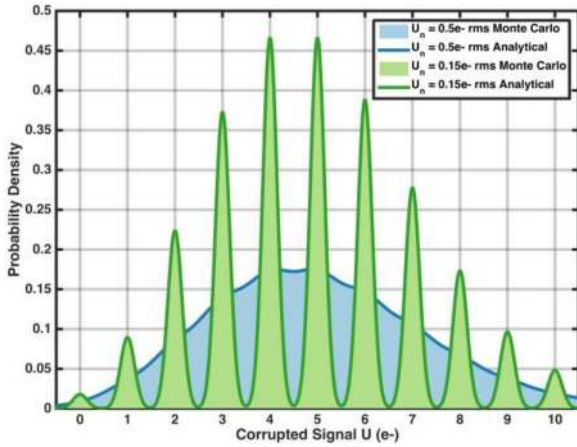
FIGURE 1. Probability density for reading corrupted signal U for quanta exposure $H = 5$ read noise $u_n = 0.15$e- rms and 0.5e- rms using the analytical equation in Eq. 1. Also shown (shaded areas) are the results of Monte-Carlo simulations for the same conditions.
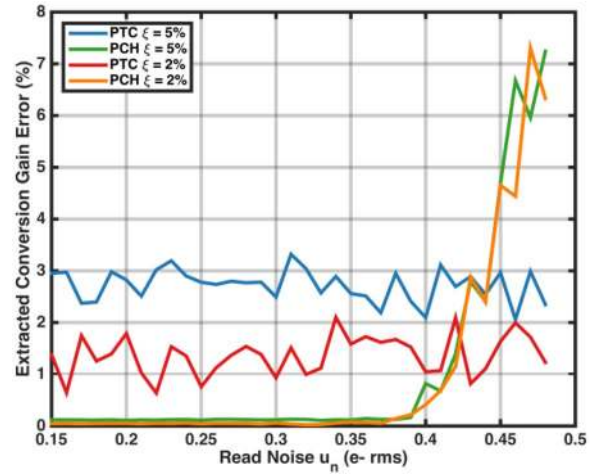

FIGURE 2. Error in calculated conversion gain as a function of read noise for both the PCH and PTC. For $0.15 < u_n < 0.40$e- rms, the PCH is more accurate than the PTC.

characterize and calibrate the device, a systematic method for extracting device parameters has yet to be developed.

In this paper, we develop a method for characterizing DSERN image sensors that is based on the photon-counting histogram and allows simultaneous characterization of read noise, quanta exposure and conversion gain.

II. PHOTON-COUNTING HISTOGRAM METHODOLOGY
A. PCH MODEL
From the model presented in [9], the probability that a single pixel will read out signal U (e-) is given by:

$$P[U] = \sum_{k=0}^{\infty} \frac{1}{u_n\sqrt{2\pi}} exp\left[\frac{-(U-k)^2}{2u_n^2}\right] \cdot \mathbb{P}[k] \qquad (1)$$

where $\mathbb{P}[k]$ is the Poisson probability mass function,

$$\mathbb{P}[k] = \frac{e^{-H}H^k}{k!} \qquad (2)$$

and where u_n is the read noise (e- rms), k is the electron number (e-), and H is the quanta exposure (e-). (The quanta exposure is the product of the integration time and the average photon or photoelectron arrival rate.) Eq. 1 is the sum of constituent probability density functions (PDF), each of which is a normal distribution with variance u_n^2 centered at electron number k and modulated by its respective Poisson probability mass function for H and k. It is essentially the convolution of the Poisson distribution with a read noise distribution.

The distribution of Eq. 1 can also be generated by Monte-Carlo simulation using a Poisson random number generator. Fig. 1 shows an example of this distribution for $u_n = 0.15$e- rms and for $u_n = 0.5$e- rms generated using either Eq. 1 or a Monte-Carlo simulation. For read noise greater than ~0.5e- rms, the quantization effect (peaks and valleys) all but disappears.

The experimentally measured PCH of a DSERN image sensor is well described by this distribution, and the analytical model or the Monte-Carlo model can be best-fit to the experimental PCH data by adjusting the parameters of quanta exposure, read noise and conversion gain while minimizing fitting error. This process can be computationally intense but yields satisfactory results. But, for most cases, quick visual inspection of the PCH can allow easy extraction of key parameters with minimal calculation, as will now be developed.

For the purpose of evaluating the parameter extraction techniques, the key parameters were used to generate synthetic experimental data via Monte-Carlo simulation. Parameters are then extracted from the synthetic data according to the techniques described below, and compared to the synthetic Monte-Carlo data input parameters to determine extraction accuracy. Based on the agreement between actual experimental PCH data in our previous work [7], [8], and the synthetic experimental PCH data, we feel confident that the methodology is sound, although we acknowledge a small danger of circular logic.

B. DETERMINING CONVERSION GAIN FROM PEAK SEPARATION
The peaks in the PCH represent quantization of electron number so their spacing can be used to quickly estimate conversion gain. During sensor characterization, the output signal is typically measured in digital numbers (DN) from the ADC output. The digital number can be converted to electrons using:

$$U = \frac{DN \cdot K}{CG} \qquad (3)$$

where DN is the digital-number-readout signal, K is the calibration constant for the analog and ADC signal chain (V/DN) and CG is the conversion gain of the sensor (V/e-). As seen in Fig. 1, each peak occurs at integer values of U

and from Eq. 3, the measured data should also have peaks that occur at certain values of *DN*. By performing a linear fit to the values of *DN* where peaks occur, *CG* can be extracted, provided one has measured the calibration constant *K*.
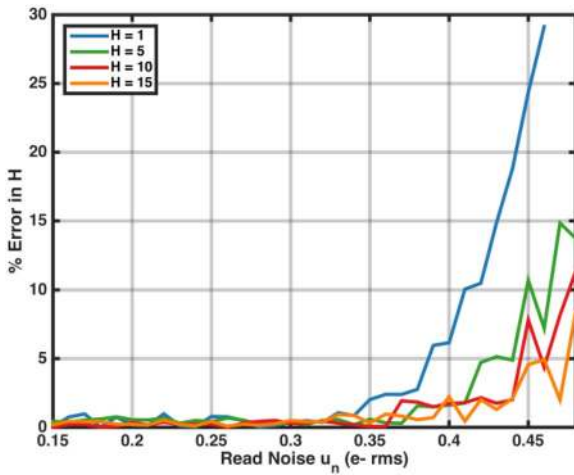

FIGURE 3. Error in calculated quanta exposure as a function of read noise. Similar trend as Fig. 2, with error increasing with read noise.

To compare the accuracy of the PCH method to that of the PTC for conversion gain extraction, a Monte-Carlo simulation was performed which simulated shot noise, read noise and non-linearity for a sensor based on the PG jot presented in [8]. To simulate the non-linearity inherent in CMOS active pixel sensors (or jots), we define the source-follower output voltage as:

$$U = CG_0 k \left(1 - \xi \frac{k}{N_{FW}}\right) \quad (4)$$

where CG_0 is the nominal conversion gain, ξ is the non-linearity coefficient, and N_{FW} is the full well capacity of the pixel in electrons. The parameter ξ effectively sets the total CG nonlinearity. The simulation results are shown in Fig. 2 for $\xi = 2\%$ and $\xi = 5\%$. To construct the PTC, simulations were conducted for $H = 1, 2, 3 \ldots 100$ and the mean and variance were calculated for each H. The mean and variance were then fitted to a straight line and the slope was taken as the conversion gain. To construct the PCH, simulations were conducted for $H = 1, 2, 3 \ldots 10$ and the conversion gain for each H was extracted. These extracted values were then averaged. Fig. 2 suggests that for values of u_n below ~0.40e- rms the PCH is a more accurate measure of the conversion gain even for a small total CG nonlinearity of 2%. It is also interesting to note that the PCH needs measurements from a single exposure to calculate both conversion gain and read noise, while the PTC method requires measurements from many exposures to obtain just the conversion gain.

C. DETERMINING QUANTA EXPOSURE FROM RELATIVE PEAK HEIGHT

The quanta exposure can be determined numerically from the PCH data, but inspection of the position of the maximum peak and the relative heights of its neighbors in the measured PCH can be used to generate a quick estimate of the quanta exposure H. A more quantitative analysis can further improve the estimate.

For a DSERN image sensor, where $u_n \leq 0.5e$- rms, the height of a peak at signal level U_p corresponding to electron number k_p in the distribution of Eq. 1 can be written as:

$$P\left[U_p\right] \cong \sum_{k=k_p-1}^{k_p+1} \frac{1}{u_n\sqrt{2\pi}} exp\left[\frac{-\left(k_p - k\right)^2}{2u_n^2}\right] \cdot \mathbb{P}[k] \quad (5)$$

and for $u_n \leq 0.35e$- rms, this equation can be further approximated by:

$$P\left[U_p\right] \cong \frac{1}{u_n\sqrt{2\pi}} \cdot \mathbb{P}[k_p] \quad (6)$$

since the peak height of each constituent PDF is mostly unaffected by the adjacent peaks at that noise level.

Considering two measured adjacent peak heights using Eq. 6, one can determine the quanta exposure H as:

$$H \cong \left(k_p + 1\right) \cdot \frac{P[U_p + 1]}{P[U_p]} \quad (7)$$

To test the validity of this approximation, a Monte-Carlo simulation was used to generate a PCH, and then the quanta exposure was extracted using Eq. 7, using the maximum peak height and that of its neighbor. Fig. 3 shows the results of the Monte-Carlo simulation. For u_n below ~0.35e- rms, Eq. 7 provides a fairly accurate measure of the quanta exposure. For larger values of u_n, the width of each peak is too large to use the simple approximation in Eq. 6. To improve the accuracy in determining H, more peak contributions can be taken into account by using Eq. 5.

D. READ NOISE FROM VALLEY-PEAK MODULATION (VPM)

As shown in Fig. 1, read noise is responsible for the loss of distinct peaks and valleys in the PCH. Since each peak is a Gaussian with width given by the read noise, a higher read noise will result in less pronounced valleys, and reduce the ratio between the peak and the valley values. This valley-peak modulation (VPM) can be used to determine the read noise. Fig. 4 shows the VPM as a function of the read noise for different H. The VPM was calculated from data generated using Eq. 1. In most cases, using Fig. 4 to graphically estimate read noise from a measured value of the VPM is sufficient. However, analytical approximations for VPM as a function of read noise can be generated that are independent of quanta exposure as shown below. Except for the simplest approximation, if the graphical method is unsatisfactory the read noise is best determined using a numerical solver tool once the VPM value is measured.

If there is a valley at signal level U_v, generally U_v will be nearly halfway between two peaks, at positions U_v- ½
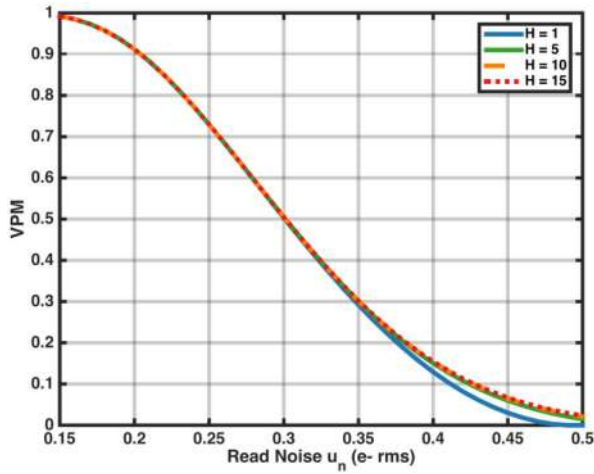
FIGURE 4. VPM as a function of read noise. For $u_n = 0.15$e- rms, the valley probability is nearly zero, so the VPM goes to 1. As u_n increases, the valley-peak ratio approaches 1, so the VPM approaches 0.

and $U_v + \frac{1}{2}$. Letting $k_p = U_v - \frac{1}{2}$ and assuming $u_n < 0.5$e-rms, we can write:

$$P[U_v] \cong \sum_{k=k_p}^{k_p+1} \frac{1}{u_n\sqrt{2\pi}} exp\left[\frac{-\left(k_p + \frac{1}{2} - k\right)^2}{2u_n^2}\right] \cdot \mathbb{P}[k] \quad (8)$$

Note only the peaks at k_p and k_p+1 are included in the summation because constituent PDFs further from the valley do not have a large influence on the resulting sum. Let $P_V \triangleq P[U_v]$ (valley PDF value) and let $P_P \triangleq \frac{1}{2}\left\{P[U_p] + P[U_p + 1]\right\}$ (average of surrounding peak PDF values). The VPM is defined as:

$$VPM = 1 - \frac{P_V}{P_P} \quad (9)$$

Using the approximations of Eqs. 5 and 8, an approximate expression for VPM for $u_n < 0.5$e- rms is:

$$VPM \cong 1 - \frac{2\ exp\left[\frac{-1}{8u_n^2}\right]}{1 + \beta \cdot exp\left[\frac{-1}{2u_n^2}\right]} \quad (10)$$

where,

$$\beta = \frac{\mathbb{P}[k_p - 1] + \mathbb{P}[k_p] + \mathbb{P}[k_p + 1] + \mathbb{P}[k_p + 2]}{\mathbb{P}[k_p] + \mathbb{P}[k_p + 1]} \quad (11)$$

If k_p and k_p+1 are chosen such that they border the center valley of the PCH then $\beta \cong 2$ (due to the pseudo-symmetry of the PCH so that $P[k_p] - P[k_p - 1] \cong P[k_p + 1] - P[k_p + 2]$, valid for $H > \sim5$) and an expression independent of H and k_p is obtained:

$$VPM \cong 1 - \frac{2exp\left[\frac{-1}{8u_n^2}\right]}{1 + 2exp\left[\frac{-1}{2u_n^2}\right]} \quad (12)$$

For $u_n < 0.35$e- rms the denominator of Eq. 12 is nearly unity and:

$$VPM = 1 - 2exp\left[\frac{-1}{8u_n^2}\right] \quad (13)$$

Another approximation was presented in [7]:

$$VPM \cong 1 - \frac{2exp\left[\frac{-1}{8u_n^2}\right] + 2exp\left[\frac{-9}{8u_n^2}\right]}{1 + 2exp\left[\frac{-1}{2u_n^2}\right]} \quad (14)$$

which is a result of extending the summation of Eq. 8 to include peaks k_p-1 and k_p+2. Fig. 5 shows a comparison between Eq. 12, 13 and 14.

To compare the accuracy of the VPM method to the dark read noise method, a Monte-Carlo simulation was performed which simulated the effects of shot noise and read noise. For the dark read noise method $H = 0$ was used to remove shot noise from the data. For the VPM method, $H = 1$, 5 and 10 was used to generate a PCH and u_n was extracted using Eq. 9 and including all peak contributions. The results are shown in Fig. 6. For $u_n < 0.45$e- rms, VPM provides a more accurate measure of read noise compared to the conventional dark read noise method.
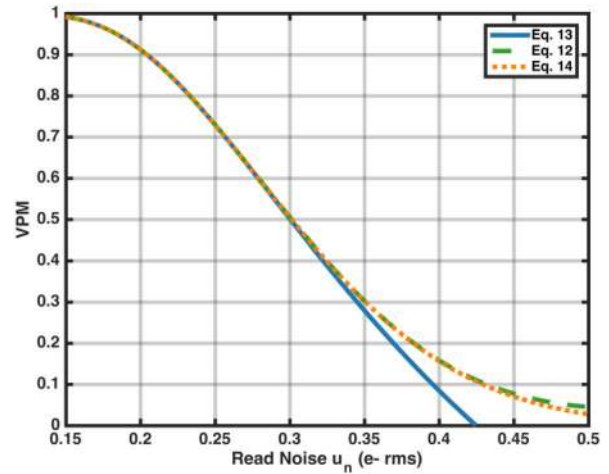

FIGURE 5. VPM as a function of read noise using Eqs. 12, 13 and 14. The plot suggests the simple approximation of Eq. 13 does not deviate far from the complicated expressions for $u_n < 0.35$e- rms.

E. CONVERSION GAIN VARIATION FROM ENSEMBLE PCH

Since Eq. 1 applies for a single pixel, the PCH of an array of pixels will have the same form with an additional source of error due to conversion gain variation. Essentially, the probability that an ensemble of pixels will readout signal U is:

$$P[U] = \sum_{k=0}^{\infty} \frac{1}{\sigma_k\sqrt{2\pi}} exp\left[\frac{-(U-k)^2}{2\sigma_k^2}\right] \cdot \mathbb{P}[k] \quad (15)$$

where

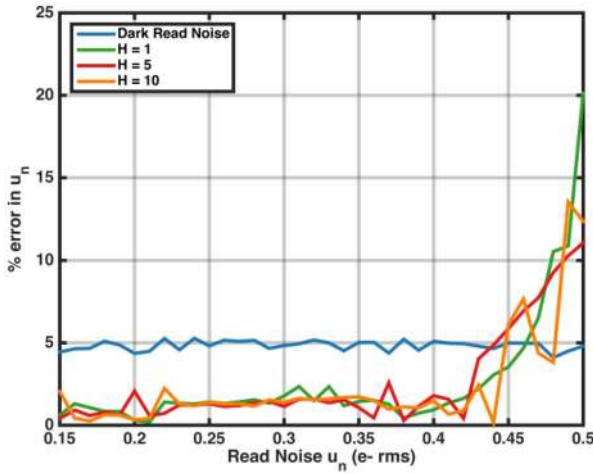$$\sigma_k^2 = u_n^2 + k^2 \left(\sigma_{CG}/\overline{CG}\right)^2 \quad (16)$$

FIGURE 6. Error in calculated read noise as a function of read noise for the dark read noise method and VPM method. For u_n < 0.45e- the VPM is more accurate than the dark read noise method.
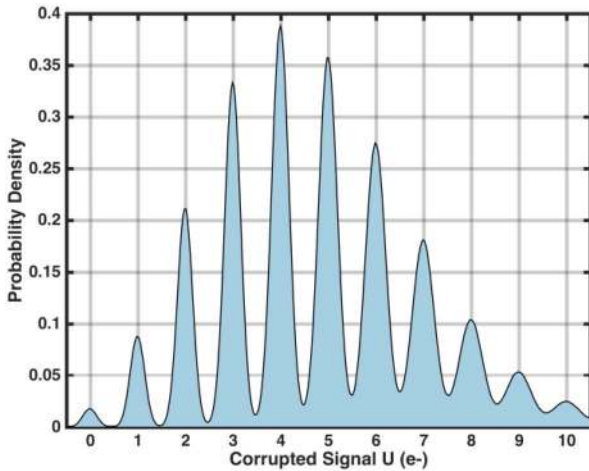

FIGURE 8. VPM as a function of electron number U for no conversion gain variation and $\sigma_{CG}/\overline{CG}$ = 2.5%. For no conversion gain variation, the VPM does not change much with electron number.

FIGURE 7. Probability density for reading corrupted signal U for quanta exposure H = 5 with read noise u_n = 0.15e- rms and $\sigma_{CG}/\overline{CG}$ = 2.5%. Since the noise is dependent on k, peaks are less distinct for higher electron numbers.

where $\overline{CG}$ and σ_{CG} are the mean and standard deviation of the conversion gain for the ensemble. A more thorough discussion is presented in [12]. The effects of conversion gain variation can be seen in Fig. 7 for $\sigma_{CG}/\overline{CG} = 2.5\%$. Fig. 8 shows the VPM for each valley for $\sigma_{CG}/\overline{CG} = 0\%$ and $\sigma_{CG}/\overline{CG} = 2.5\%$. For no conversion gain variation, there is little change in the VPM, while the VPM for $\sigma_{CG}/\overline{CG} = 2.5\%$ drops off due to the k-dependent noise.

The VPM presented in Section II-D can still be applied to this ensemble PCH, but instead the VPM for each valley is used. From the VPM v. U data in Fig. 8, a σ_k can be calculated for each valley. The read noise of the ensemble can be easily calculated, since for $k = 0$, $\sigma_k = u_n$. Furthermore, from Eq. 16, if a linear fit is performed to a plot of σ_k^2 vs. k^2 the slope will be $(\sigma_{CG}/\overline{CG})^2$.

To test the accuracy of this methodology, Monte-Carlo PCH simulations were conducted on a 200x200 array of
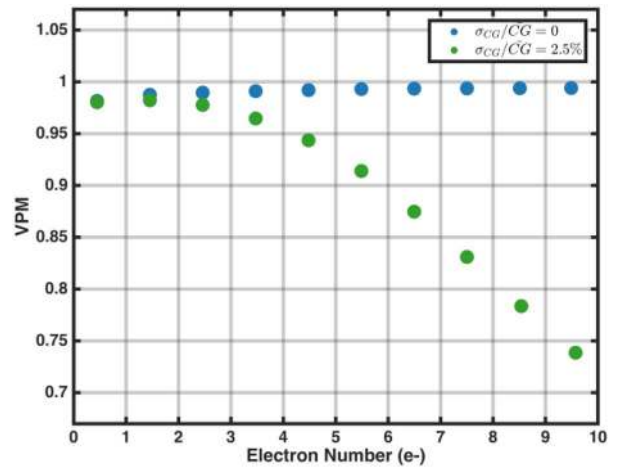
pixels for different conversion gain variations, and then $\sigma_{CG}/\overline{CG}$ was extracted from the PCHs. The results are shown in Fig. 9. The VPM v. U method seems to yield a good measure of the conversion gain variation. However, for higher conversion gain variation, there is an increase in the error in the calculated read noise.

F. DATA REQUIREMENTS
For the Monte-Carlo simulations presented in the previous sections, the sensor under test was a 200x200 pixel array that was simulated 100 times for a total of 4,000,000 samples. To investigate how the number of samples affects the error in the extracted parameters, multiple PCHs were synthetically constructed using the same 200x200 pixel array each with a different number of runs. Then, conversion gain, quanta exposure and read noise were calculated for each PCH and the percent error was determined. When a smaller number of runs are used, both the peak height and location in the PCH will shift leading to errors in the calculated parameters. The percent error in conversion gain was found to be flat for all number of samples, likely because the conversion gain only uses the location of each peak. The number of runs also had little effect on the error in read noise. For extracting the quanta exposure, with less runs, there was a slight increase in error.

III. DATA EXTRACTION EXAMPLE
A. SAMPLE EXTRACTION FOR TPG JOT
In this section, an example calculation for a TPG jot described in [8] is presented. Fig. 10 shows the experimental PCH from the sensor. To generate the PCH, a single pixel was readout 200,000 times and a histogram was constructed from the resulting data. The first step of the extraction, depending on the number of samples used to construct the PCH, is to smooth the data with a smoothing spline so that the automated extraction code does not get stuck during the
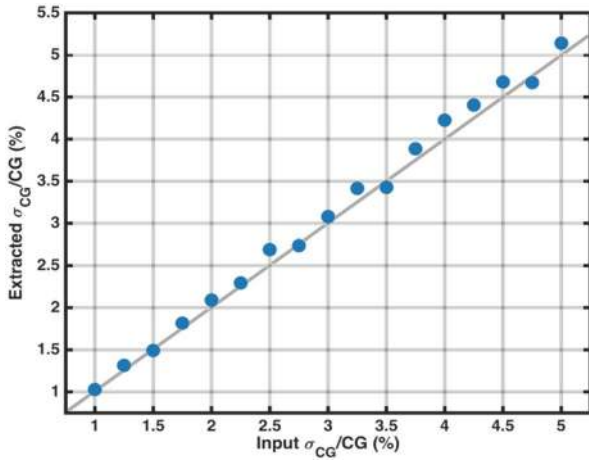
FIGURE 9. Conversion gain variation extraction from synthetic PCH data using VPM v. *U* method, showing good agreement between input parameter and extracted parameter.
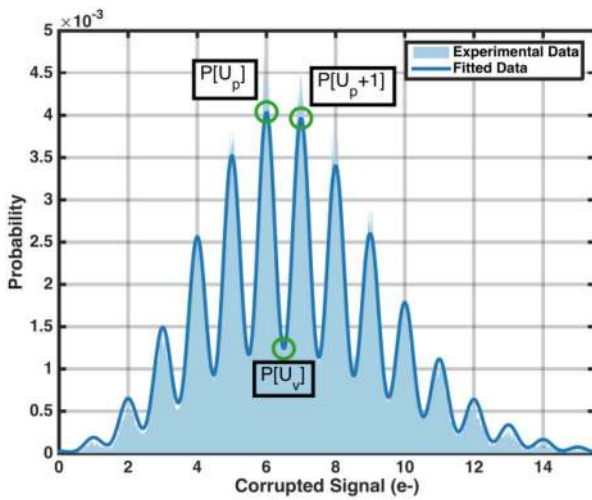

FIGURE 10. Sample data from a TPG jot presented in [8]. The experimental data and fitted curve show good agreement (see Section III-A for extracted parameters). The peaks and valleys are labeled for reference.

computation. Next, the conversion gain needs to be calculated, so the data can be converted from DN to e-. This is done by calculating the location and probability of each peak and fitting the location data to a straight line. The resulting slope is the conversion gain in e-/DN. The value of the conversion gain in μV/e- is obtained by using K, the analog and ADC signal chain calibration constant (see Eq. 3). For this example, the extracted conversion gain is 417μV/e-. The quanta exposure and read noise are not needed to calculate the conversion gain.

Next, the quanta exposure is calculated after the data has been converted from DN to e-. From Eq. 7 only the peak probability for k_{max} and $k_{max}+1$ as well as the location of k_{max} is needed to determine the quanta exposure. Using the peak locations and probabilities calculated in the previous step, the exposure can be calculated resulting in a quanta exposure of 6.87e-.

Finally, the read noise is calculated using the VPM. From Eq. 10 the only additional piece of information needed is the location and probability for the valley that is between k_{max} and $k_{max}+1$. This is straightforward since the location and probability of the two neighboring peaks is already known. Using Fig. 4, one can simply read off the value of the read noise based on the VPM. The read noise for this example is 0.26e- rms. Alternatively, to calculate the read noise, Eq. 10 can be solved for u_n using a zero finder. Fig. 10 shows the fitted curve overlaid on the original data and illustrates the accuracy of the extracted parameters.

IV. CONCLUSION

In this paper, a new method of characterizing DSERN image sensors is reported based on the photon-counting histogram (PCH). The accuracy in extracted parameters was determined using synthetic PCH data. With the push towards photon counting image sensors, this method will be beneficial for characterizing next generation DSERN image sensors, and has already been successfully used by others [13].

ACKNOWLEDGMENT

REFERENCES

[1] J. R. Janesick, J. Hynecek, and M. M. Blouke, "Virtual phase imager for Galileo," *Solid State Imagers Astron.*, vol. 290, pp. 165–174, Jun. 1981.

[2] L. Mortara and A. Fowler, "Evaluations of charge-coupled device (CCD) performance for astronomical use," in *Proc. SPIE*, vol. 290. Cambridge, U.K., Jan. 1981, pp. 28–33.

[3] B. P. Beecken and E. R. Fossum, "Determination of the conversion gain and the accuracy of its measurement for detector elements and arrays," *J. Opt. Soc. America*, vol. 35, no. 19, pp. 3471–3477, 1996.

[4] J. Janesick, K. Klaasen, and T. Elliott, "CCD charge collection efficiency and the photon transfer technique," in *Proc. 29th Annu. Tech. Symp. Int. Soc. Opt. Photon.*, San Diego, CA, USA, 1985, pp. 7–19.

[5] N. A. W. Dutton, L. Parmesan, A. J. Holmes, L. A. Grant, and R. K. Henderson, "320×240 oversampled digital single photon counting image sensor," in *Symp. VLSI Technol. Dig. Tech. Papers*, Honolulu, HI, USA, Jun. 2014, pp. 1–2.

[6] J. Ma and E. R. Fossum, "A pump-gate jot device with high conversion gain for a quanta image sensor," *IEEE J. Electron Devices Soc.*, vol. 3, no. 2, pp. 73–77, Mar. 2015.

[7] J. Ma and E. R. Fossum, "Quanta image sensor jot with sub 0.3e- r.m.s. read noise and photon counting capability," *IEEE Electron Device Lett.*, vol. 36, no. 9, pp. 926–928, Sep. 2015.

[8] J. Ma, D. Starkey, A. Rao, K. Odame, and E. R. Fossum, "Characterization of quanta image sensor pump-gate jots with deep sub-electron read noise," *IEEE J. Electron Devices Soc.*, vol. 3, no. 6, pp. 472–480, Nov. 2015.

[9] E. R. Fossum, "Modeling the performance of single-bit and multi-bit quanta image sensors," *IEEE J. Electron Devices Soc.*, vol. 1, no. 9, pp. 166–174, Sep. 2013.

[10] P. Finocchiaro *et al.*, "Characterization of a novel 100-channel silicon photomultiplier—Part II: Charge and time," *IEEE Trans. Electron Devices*, vol. 55, no. 10, pp. 2765–2773, Oct. 2008.

[11] S. Wolfel *et al.*, "Sub-electron noise measurements on RNDR devices," in *Proc. IEEE Nuclear Sci. Symp. Conf. Rec.*, vol. 1. San Diego, CA, USA, Oct. 2006, pp. 63–69.

[12] E. R. Fossum, "Photon counting error rates in single-bit and multi-bit quanta image sensors," *IEEE J. Electron Devices Soc.*, to be published.

[13] M.-W. Seo, S. Kawahito, K. Kagawa, and K. Yasutomi, "A 0.27e-rms read noise 220-μV/e- conversion gain reset-gate-less CMOS image sensor with 0.11-μm CIS process," *IEEE Electron Device Lett.*, vol. 36, no. 12, pp. 1344–1347, Dec. 2015.

ERIC R. FOSSUM (S'80–M'84–SM'91–F'98) is currently a Professor with the Thayer School of Engineering at Dartmouth. He is the primary inventor of the CMOS image sensor used in smartphones and other applications. He is currently exploring the quanta image sensor. He is the Co-Founder and the Past President of the International Image Sensor Society and the Director of the National Academy of Inventors. He was inducted into the National Inventors Hall of Fame and is a member of the National Academy of Engineering.

DAKOTA A. STARKEY (S'15) received the B.A. degree in physics from Vassar College, Poughkeepsie, NY, USA, in 2013, and the B.E. degree in electrical engineering from Dartmouth College, Hanover, NH, USA, in 2014, as part of a dual degree program. He is currently pursuing the Ph.D. degree with the Thayer school of Engineering at Dartmouth. His research focus is developing the quanta image sensor (QIS) with emphasis on low-power, high-speed readout circuit design, and QIS applications.